Hybrid optimal control of dry clutch engagement

Heijden, A.C. van der; Serrarens, A.F.A.; Camlibel, M.K.; Nijmeijer, H.

Published in:
International Journal of Control

Publication date:
2007

International Journal of Control
Vol. 80, No. 11, November 2007, 1717–1728

Taylor & Francis
Taylor & Francis Group

Hybrid optimal control of dry clutch engagement

A. C. VAN DER HEIJDEN*†, A. F. A. SERRARENS‡,
M. K. CAMLIBEL† and H. NIJMEIJER†

†Department of Mechanical Engineering, Eindhoven University of Technology,
PO Box 513, 5600 MB Eindhoven, The Netherlands
‡Drivetrain Innovations BV, Croy 46, 5653 LD Eindhoven, The Netherlands

(*Received 11 July 2006; in final form 2 February 2007*)

Lately, with the increasing use of automated manual transmissions (AMT) the engagement control of the dry clutch becomes more important. The engagement control plays a crucial role, since different and conflicting objectives have to be satisfied: preservation of driver comfort, fast engagement and small friction losses. In this paper two optimal control strategies for clutch engagement, based on hybrid control principles, are compared. For developing a useful clutch control scheme, the driveline is modelled as a piecewise linear system. The first control strategy is widely known as explicit MPC. However, it seems that it is not suitable (yet) for this type of problem. The second strategy is a piecewise LQ controller, based on piecewise quadratic Lyapunov functions. Simulation results obtained with both strategies are presented and discussed.

1. Introduction

Lately, the use of automated manual transmissions (AMT) is increasing. The main reason for this is that AMTs are an inexpensive add-on solution to classical manual transmissions, while improving driver comfort. A crucial role in AMT transmissions is played by the engagement of the dry clutch, since the powertrain performance depends heavily on it. This is especially the case at a start-up from standstill, the so-called ''vehicle launch''.

The clutch engagement must be controlled in order to satisfy different and conflicting objectives: preservation of driver comfort, fast engagement and small friction losses. As a result of this, the engagement control of automotive dry clutches is becoming more and more important.

Many different approaches for control of dry clutch engagement have already been investigated in the literature. In Serrarens *et al.* (2004) a decoupling PI controller is proposed. In Glielmo and Vasca (2000) the authors have proposed a finite horizon linear quadratic (LQ) feedforward-feedback controller as a solution for the dry clutch engagement problem. Observer-based optimal control is discussed in Dolcini *et al.* (2005). In Bemporad *et al.* (2001a,b) a model predictive control (MPC) strategy was proposed. The explicit solution for this controller can be calculated off-line by using various mathematical programming techniques, thereby avoiding the computational drawbacks of classical MPC strategies. The proposed MPC controller, however, does not take driveline dynamics and comfort issues explicitly into account. It is therefore desired to design a controller that does exhibit such properties. In this paper two different optimal control strategies for dry clutch engagement are investigated, both of which are based on hybrid control principles.

The outline of this paper is as follows. In § 2, the modelling of an automotive powertrain is discussed. In § 3, the control objectives are stated. Subsequently, the design of an explicit MPC and a PWLQ controller are discussed. Both controllers are evaluated by means of simulation, and results are discussed in § 4. Finally, conclusions are drawn in § 5.

*Corresponding author. Email: a.c.v.d.heijden@student.tue.nl

International Journal of Control
ISSN 0020–7179 print/ISSN 1366–5820 online © 2007 Taylor & Francis
http://www.tandf.co.uk/journals
DOI: 10.1080/00207170701473995

2. Powertrain modelling

In general, passenger car powertrains consist of the following basic elements:

- internal combustion engine;
- launch device;
- gearbox and differential;
- drive shafts.

The powertrain considered in this specific case is equipped with an automated manual transmission (AMT) and a dry friction clutch that is used as a launch device. This is depicted schematically in figure 1. In this section the physical modelling of these elements will be discussed. For simulation and validation of the controllers it is necessary to consider the tyre-road behaviour and the longitudinal dynamics of the vehicle as well.

Physical modelling of powertrains is already well covered in the literature, among others in Serrarens *et al.* (2004) and references contained therein.

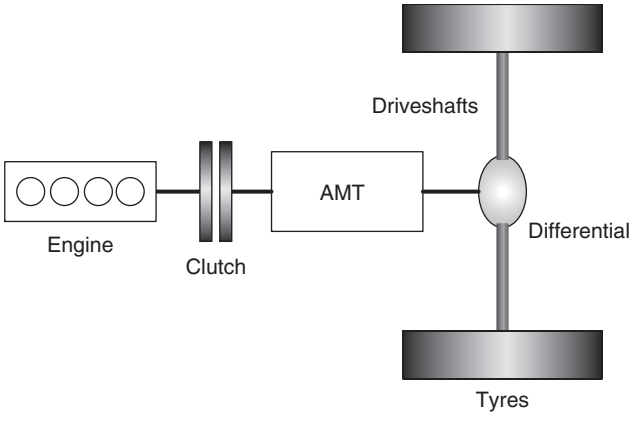

Figure 1. Schematic overview of the powertrain.

2.1 *Engine*

The engine can be modelled as a rotating rigid body with inertia J_e. The torque T_e represents the net torque generated by the engine, considering also friction and torque losses. It is assumed that this torque can be prescribed and it is henceforth considered as a control input. The generated torque is positive valued and upper bounded by a certain maximum value, dependent on the engine speed ω_e. This follows from the engine characteristic. For the investigation on the clutch engagement process the high frequency vibrations of the engine, resulting from the combustion process, can be neglected.

2.2 *Dry friction clutch*

The clutch system, shown in figure 2, consists of a housing, pressure plates, friction plates, a clutch disc with torsion dampers and a release mechanism. The clutch disc is mounted onto the transmission input shaft and is radially fixed by a splined interface. The clutch is normally closed, as the diaphragm spring is pre-tensioned when assembled. The axial bearing can slide over the transmission input shaft and push against the fingers of the diaphragm spring. The direction of the release force is swapped through the lever joints and releases the pressure from the clutch disc, which is then able to rotate independently from the engine.

Furthermore, the clutch disc is equipped with torsional 'dampers', which consist of a complex assembly of coil springs in parallel and series. These springs aim at maximizing the driver comfort during (dis)-engagement of the clutch and can be modelled as a spring with piecewise linear stiffness (Serrarens *et al.* 2004). The torque transmitted through the clutch is denoted by T_c.

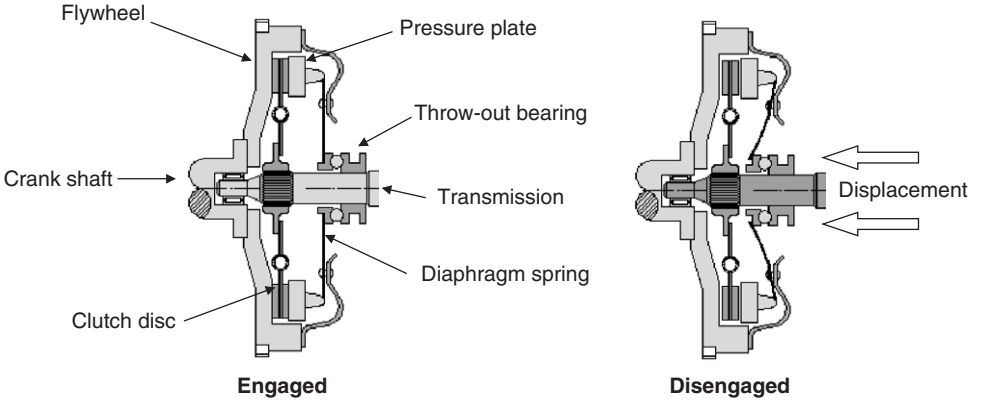

Figure 2. Schematic overview of a dry clutch.

2.2.1 Slipping clutch. Assuming a Coulomb friction model, the torque through the clutch during slipping is given by

$$T_c = F_n \mu R_a \text{sign}(\omega_e - \omega_c). \tag{1}$$

Here F_n is the actuation force working on the clutch disc, μ the dynamic friction coefficient of the clutch surface material, R_a the effective radius of the clutch disc and ω_c the rotational speed of the clutch disc.

2.2.2 Sticking clutch. When the clutch is sticking, the engine is rigidly coupled to the driveline. Consequently, the two equations of motion of the engine and the clutch are merged into a single equation. Moreover, during sticking the torque through the clutch cannot be altered by the actuator force F_n anymore. Instead of a ''controlled'' input, it becomes a ''constrained'' variable. This is discussed in more detail in § 3.2.

The switch from the slipping model to the engaged model is determined by the equality condition $\omega_e = \omega_c$ with the constraint that the clutch torque is smaller than the static friction torque

$$-F_n \mu_0 R_a \leq T_c \leq F_n \mu_0 R_a, \tag{2}$$

where μ_0 is the static friction coefficient of the clutch.

2.3 *Gearbox, differential and drive shafts*

The gearbox input shaft is connected to the friction plate of the clutch. The output shaft is driven by the input shaft through a gear mesh and is connected to the differential via the final drive. The overall transmission ratio is given by

$$\omega_c = i_{\text{tot}} \omega_d \tag{3}$$

with i_{tot} the overall transmission ratio and ω_d the rotational speed of the output gear of the final drive. Backlash of the gears is neglected. Power losses in the gearbox and differential can be modelled as a damper to the fixed world, but these will not be taken into account for this research. Instead, an efficiency of 100% is assumed.

The drive shafts connect the differential to the wheels. Since only straight line driving is considered, the two drive shafts are lumped into one a single stiffness k_s with damping b_s.

2.4 *Tyres and vehicle*

The drive torque T_s is transmitted onto the road via the tyres, resulting in longitudinal acceleration of the vehicle. The governing equations of motion are given by

$$J_w \dot{\omega}_w = T_s - R_w F_x - R_w F_{\text{roll, front}} \tag{4}$$

$$m_v \dot{v}_v = F_x - (F_{\text{air}} + F_{\text{roll, rear}} + F_{\text{incl}}) \tag{5}$$

with J_w the wheel inertia, ω_w the rotational speed of the wheels, R_w the dynamic wheel radius, m_v the vehicle mass, v_v the vehicle speed and F_x the tyre friction force, defined as

$$F_x = F_z \mu(\kappa, \alpha, F_z) \tag{6}$$

where tyre friction coefficient $\mu(\kappa, \alpha, F_z)$ is a non-linear function dependent on the longitudinal slip κ, side slip angle α and tyre vertical load F_z. The most common tyre friction model used in the literature is the so-called Magic Formula or Pacejka model (Pacejka 2002), which uses static maps to describe the relation between slip and friction.

Furthermore, F_{air}, $F_{\text{roll, (front/rear)}}$, F_{incl} are additional load forces due to air resistance, rolling resistance and road inclination, respectively. These are given by

$$F_{\text{air}} = \left(\frac{1}{2}\right) \rho c_w A \dot{v}_v^2 \tag{7}$$

$$F_{\text{roll, (front/rear)}} = f_r F_{z, \text{(front/rear)}} \tag{8}$$

$$F_{\text{incl}} = m_v g \sin \gamma \tag{9}$$

with ρ the air density, c_w the air resistance coefficient, A the frontal area of the vehicle, f_r the rolling resistance coefficient, g the gravitation, γ the road inclination angle. Regarding the rolling resistance, a distinction is made between front (driving) and rear (driven) wheels, assuming front-wheel drive.

3. Controller design

3.1 *Objectives*

The control objective is stated as follows. ''Specify an input force, and/or an engine torque, as function of a desired vehicle acceleration, that results in a smooth, though fast engagement of the clutch. The clutch engages smoothly if the vehicle acceleration has a continuous and preferably non-negative derivative after the clutch sticks''.

Engaging the clutch too fast can result in stall of the engine, tyre slip and torsional excitation of the driveline, all of which make for an uncomfortable experience for the driver. On the other hand, excessive slipping of the

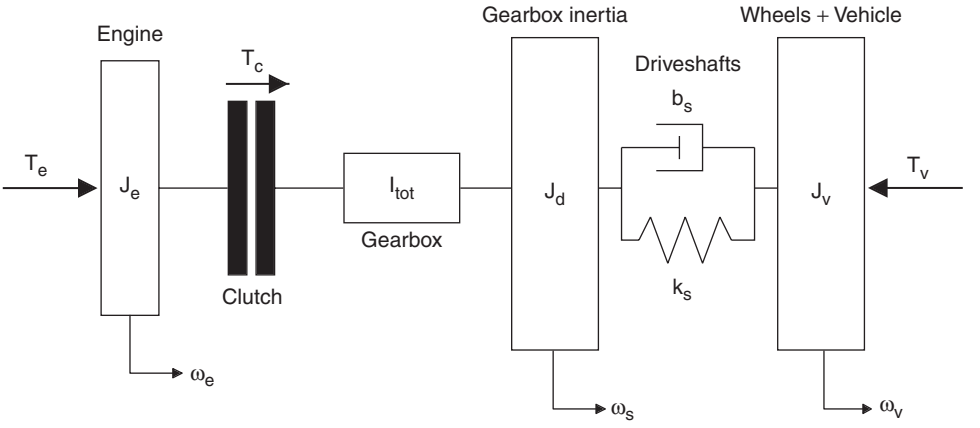

Figure 3. Schematic overview of the simplified powertrain model.

Table 1. Model parameters.

Parameter	Value	Unit
J_e	0.184	$\mathrm{kg\,m^2}$
J_d	1.1828	$\mathrm{kg\,m^2}$
J_v	91.76	$\mathrm{kg\,m^2}$
J_w	1.35	$\mathrm{kg\,m^2}$
k_s	6000	Nm/rad
b_s	42	Nms/rad
R_w	0.281	m
i_{tot}	13.894	–
μ	0.2	–
τ	0.1	s

clutch should be prevented in order to minimize wear and heat build up. Therefore, in designing the controller, the following requirements are to be considered:

- minimize the clutch lock-up time;
- prevent stalling of the engine;
- minimize the energy dissipated during the slipping phase;
- ensure a smooth acceleration of the vehicle.

3.2 *Reduced model for control*

For the purpose of controller design a simplified powertrain model is used. This is especially important when using the explicit MPC technique, since the complexity of the solution depends heavily on the number of state variables. Next, the simplified model is described.

The most important assumption is that the wheel inertia and equivalent vehicle inertia are lumped (i.e., slipping of the tyres is neglected) into one inertia J_v, given by

$$J_v = m_v R_w^2 + J_w. \tag{10}$$

The motivation for this simplification is that it is very difficult to characterize the non-linear tyre slip forces during vehicle launch with simple linear expressions. Furthermore, the clutch springs are also neglected, since these have a relatively large stiffness. Gear shifting is not considered and all rotating transmission parts are assumed to be lumped in one equivalent inertia $J_d(i_{\mathrm{tot}})$. The simplified model is depicted in figure 3. The dynamics during slipping can then be described by the following equations:

$$J_e\dot{\omega}_e = T_e - T_c \tag{11}$$

$$\frac{J_d(i_{\mathrm{tot}})}{i_{\mathrm{tot}}}\dot{\omega}_c = i_{\mathrm{tot}}T_c - T_s - b_s(\omega_d - \omega_v) \tag{12}$$

$$J_v\dot{\omega}_v = T_s + b_s(\omega_d - \omega_v) - T_v \tag{13}$$

$$\dot{T}_s = k_s(\omega_d - \omega_v). \tag{14}$$

With the clutch torque T_c given by (1). The additional load T_v, due to air resistance, roll resistance and road inclination (as described in § 2.4), is considered to be small at low vehicle velocities (i.e., vehicle launch) and hence it is neglected.

During sticking we have $\omega_e = \omega_c$. This reduces (11) and (12) into a single equation

$$\left(\frac{i_{\mathrm{tot}}^2 J_e + J_d}{i_{\mathrm{tot}}}\right)\dot{\omega}_e = i_{\mathrm{tot}}T_e - T_s - b_s(\omega_d - \omega_v). \tag{15}$$

The clutch torque during the sticking phase can be found by combining (11) and (12) and is given by

$$T_c = \frac{J_d T_e + i_{\mathrm{tot}} J_e\big(T_s + b_s(\omega_d - \omega_v)\big)}{i_{\mathrm{tot}}^2 J_e + J_d}. \tag{16}$$

Values of the used parameters are reported in table 1.

3.3 *Explicit model predictive control*

The general optimization problem used in the MPC strategy (with a linear performance index) is given by (Kvasnica *et al*. 2004)

$$\begin{aligned}\min & \left\| P_N\big(x(N)-x_{\text{ref}}\big)\right\|_\infty \\ & + \sum_{k=0}^{N-1} \left\| Q\big(x(k)-x_{\text{ref}}\big)\right\|_\infty + \|R\Delta u(k)\|_\infty \\ \text{s.t. } & x(k+1) = A_{d,i}x(k) + B_{d,i}u(k) \\ & u_{\min} \le u(k) \le u_{\max} \\ & \Delta u_{\min} \le u(k) - u(k-1) \le \Delta u_{\max} \\ & x_{\min} \le x(k) \le x_{\max}.\end{aligned} \tag{17}$$

The matrices P_N, Q and R penalize the final state, the states and the inputs, respectively, $\|Vx\|_\infty \triangleq \max_{i=1,\ldots,m}(V^{\{i\}}x)$, and $V^{\{i\}}$ is the ith row of a generic matrix $V \in \mathbb{R}^{r\times m}$.

The traditional implementation of MPC then uses on-line optimization to compute the optimal control inputs ahead in time for a fixed number of samples. However, this is not possible for fast systems since there is simply not enough time to complete the on-line optimization process.

Therefore, it was proposed to solve the optimization problem parametrically (Bemporad *et al*. 2000). This results in a large set of explicit piecewise affine control laws and reduces on-line computation to a simple linear function evaluation. However, the complexity of the solution of the optimization problem depends heavily on the number of PWA modes, state variables and control inputs as well as on the length of the prediction horizon.

The design of the controller is performed in two steps. First, the optimal control law is tuned in simulation until the desired performance is achieved. Finally, the PWA explicit version is calculated. Both steps are done with the help of the MPT Toolbox (Kvasnica *et al*. 2004).

It should be noted that from a control point of view it is more desirable to use a quadratic performance index, but these type of problems are in general much harder to solve, both for on-line and for explicit MPC.

Based on the model discussed in § 3.2, the state and input variables are chosen to be

$$x = \begin{pmatrix} \omega_e \\ (\omega_e - \omega_c) \\ \left(\dfrac{\omega_c}{i_{\text{tot}}} - \omega_v\right) \\ T_s \end{pmatrix}, \quad u = \begin{pmatrix} T_c \\ T_e \end{pmatrix} \tag{18}$$

resulting in the following state space representation:

$$\dot{x} = \begin{cases} A_1 x + B_1 u, & \text{if } x_1 > \eta \\ A_2 x + B_2 u, & \text{if } |x_1| < \eta, \end{cases} \tag{19}$$

where switching boundary η is a small-valued constant that defines a "stick band", which approximates the stick mode. The state space matrices are given by equations (20)–(22).

Slip:

$$\begin{aligned} A_1 &= \begin{pmatrix} 0 & 0 & 0 & 0 \\ 0 & 0 & \dfrac{b_s i_{\text{tot}}}{J_d} & \dfrac{i_{\text{tot}}}{J_d} \\ 0 & 0 & -\dfrac{b_s}{J_d} - \dfrac{b_s}{J_v} & -\dfrac{1}{J_d} - \dfrac{1}{J_v} \\ 0 & 0 & k_s & 0 \end{pmatrix}, \\ B_1 &= \begin{pmatrix} -\dfrac{1}{J_e} & \dfrac{1}{J_e} \\ -\dfrac{1}{J_e} - \dfrac{i_{\text{tot}}^2}{J_d} & \dfrac{1}{J_e} \\ \dfrac{i_{\text{tot}}}{J_d} & 0 \\ 0 & 0 \end{pmatrix} \end{aligned} \tag{20}$$

Stick:

$$\begin{aligned} A_2 &= \begin{pmatrix} 0 & 0 & -\dfrac{b_s i_{\text{tot}}}{J_{\text{tot}}} & -\dfrac{i_{\text{tot}}}{J_{\text{tot}}} \\ 0 & 0 & 0 & 0 \\ 0 & 0 & -\dfrac{b_s}{J_{\text{tot}}} - \dfrac{b_s}{J_v} & -\dfrac{1}{J_{\text{tot}}} - \dfrac{1}{J_v} \\ 0 & 0 & k_s & 0 \end{pmatrix}, \\ B_2 &= \begin{pmatrix} 0 & \dfrac{i_{\text{tot}}^2}{J_{\text{tot}}} \\ 0 & 0 \\ 0 & \dfrac{i_{\text{tot}}}{J_{\text{tot}}} \\ 0 & 0 \end{pmatrix}, \end{aligned} \tag{21}$$

where

$$J_{\text{tot}} = J_e i_{\text{tot}}^2 + J_d. \tag{22}$$

The reduced model (19) is discretized in time with sampling period $t_s = 0.01$ [s].

The constraints on the optimization problem (17) originate from actual physical constraints, with $\omega_e \ge \omega_{e,min}$ (the minimum engine speed), $\omega_c \ge 0$ (the minimum slip speed), $u_{\min} = [0, 0]$, $u_{\max} = [T_{c,\max}, T_{e,\max}]$ (the minimum and maximum values of the clutch and the engine torque), $\Delta u_{\min} = [\Delta T_{c,\min}, \Delta T_{e,\min}]$, $\Delta u_{\max} = [\Delta T_{c,\max}, \Delta T_{e,\max}]$ (the minimum and maximum values of the torque increments at each step).

3.3.1 Tuning. The parameters of the controller to be tuned are the horizon length N and the weights Q and R. By increasing the prediction horizon N the controller performance improves, but at the same time the number of constraints in the optimization problem increases. This will there upon lead to a dramatic increase of the complexity of the final PWA explicit controller. Choosing N therefore comes down to finding the smallest N which leads to a satisfactory closed-loop behaviour. A satisfactory performance was achieved with

$$N = 2, \quad Q = \begin{bmatrix} 0 & 0 & 0 & 0 \\ 0 & 1 & 0 & 0 \\ 0 & 0 & 300 & 0 \\ 0 & 0 & 0 & 0.1 \end{bmatrix}, \quad R = \begin{bmatrix} 0 & 0 \\ 0 & 0 \end{bmatrix},$$

resulting in a PWA controller consisting of 6812 regions with 229 different control laws. Note that no penalties are placed on the control effort. This is not a problem, since the control effort is already restricted by the constraints.

Due to the computationally intensive nature of these problems, it was unfortunately not possible to calculate an explicit controller with a longer horizon. However, it is possible to simulate on-line controllers with longer horizons. To get a better feeling for the influence of the length of the prediction horizon an on-line MPC controller with an increased prediction horizon of 50 steps (using the same weights), was also simulated. Surprisingly, this resulted in more or less the exact same responses as those obtained using a controller with $N = 2$. This can be explained by the fact that with the original controller the system is already running on the bounds of the allowable operating conditions, always restricted by one or more constraints. It should be noted that the event of clutch stick (i.e. mode switching) is not contained within the 50 prediction steps. An even larger prediction horizon that would take this mode switch into account could therefore lead to an entirely different behaviour. However, it is almost impossible to run simulations with a prediction horizon this long, so this could not be verified.

3.3.2 Simulation results. The controller designed in the previous section has been tested in simulation on the extended vehicle model. This model incorporates the clutch torsion damper, as well as a simple tyre model and external loads, as described in §2. Simulink with SimDriveline (Mathworks. Inc. 2005) was used for this purpose. Simulation results obtained with the PWA MPC controller are depicted in figure 4.

It can be observed that lock-up of the clutch is achieved at approximately 0.8 seconds. The drive torque increases sufficiently smooth. It can also be observed that the engagement process can roughly be divided in three stages: (1) first, the engine rotational speed is brought down as quickly as possible, until it reaches the lower bound that is specified for it. Meanwhile, the clutch is speeding up; (2) the clutch is still speeding up as fast as possible, where the maximum acceleration is bounded by the maximum increment of the clutch torque (i.e., the clutch normal force); (3) when the clutch sticks, the load on the engine increases as it is rigidly coupled with the driveline from that point. It can also be observed that only very few controller regions are actually used.

Simulations to test the controller against model variations and disturbances were also carried out. It was noticed that model variations or disturbances very often lead to infeasibility of the controller, especially when the control inputs T_c and T_e are subject to small disturbances (e.g., due to modelled limitations of the actuator(s)).

3.4 *Piecewise linear quadratic control*

Since MPC has some serious drawbacks (computationally demanding, sensitive to disturbances and model variations) it is proposed to use the piecewise linear quadratic optimal control technique along the lines of Rantzer and Johansson (2000) and Johansson (1999) to construct a controller. This technique suggests searching for piecewise quadratic Lyapunov functions using convex optimization. The key idea is to make the piecewise Lyapunov function continuous across the region boundaries.

Consider piecewise affine systems of the form

$$\dot{x}(t) = A_i x(t) + a_i + B_i u(t), \quad x(t) \in X_i \tag{23}$$

with $\{X_i\}_{i \in I} \subseteq \mathbb{R}^n$ a partition of the state space into a number of closed polyhedral cells. The index set of the cells is denoted by I. Furthermore, for each polyhedral cell a matrix $\bar{E}_i$ can be constructed, such that

$$\bar{E}_i \begin{bmatrix} x \\ 1 \end{bmatrix} \geq 0, \quad x \in X_i, \quad i \in I. \tag{24}$$

This inequality means that each entry of the vector on the left hand side is non-negative.

The control problem is to bring the system to $x(\infty) = 0$ from an arbitrary initial state $x(0)$, while minimizing the cost

$$J(x_0, u) = \int_0^\infty \left(x^T Q_i x + u^T R_i u\right) \mathrm{d}t. \tag{25}$$

Here, the matrices Q_i and R_i penalize the states and the inputs, respectively.

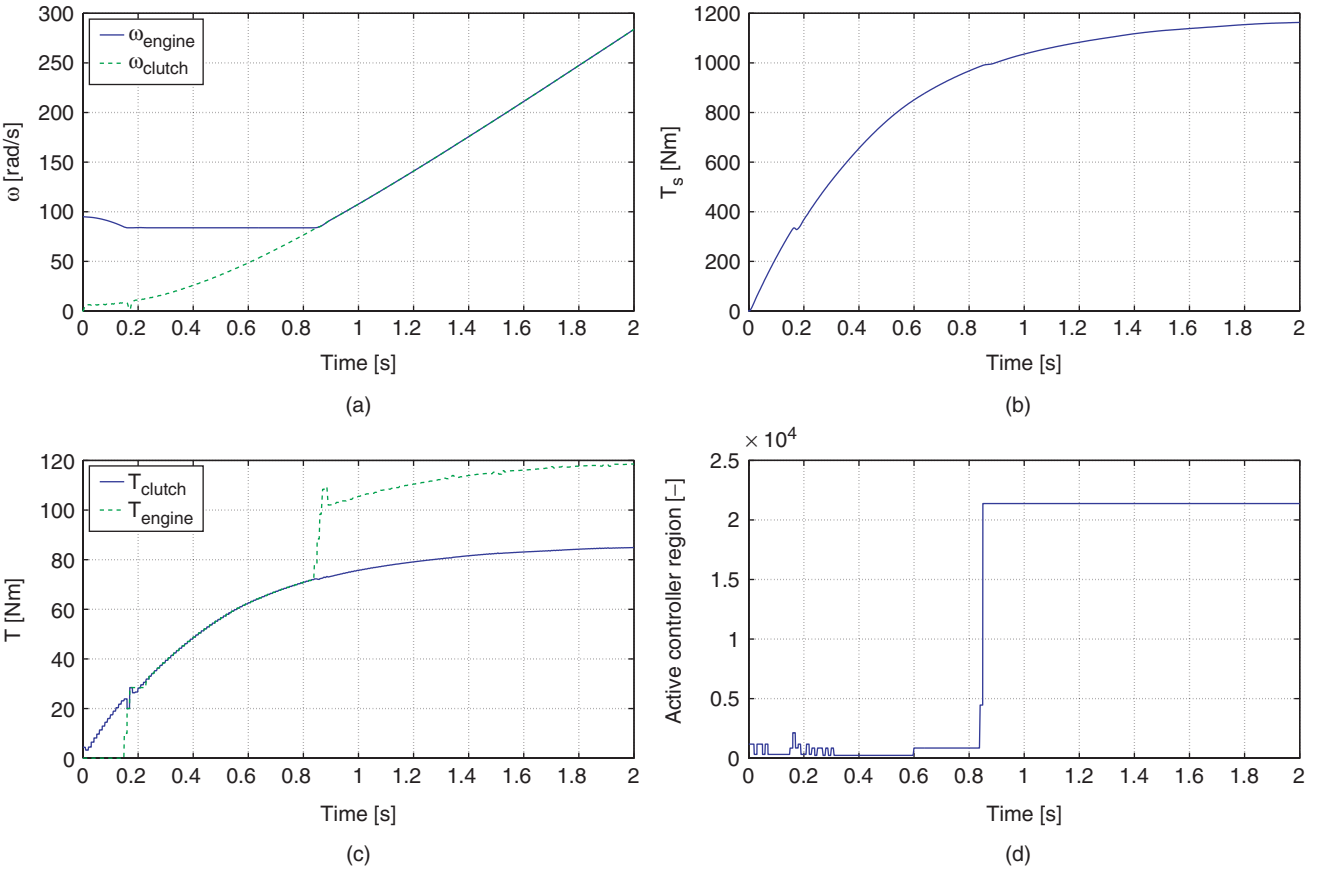

Figure 4. Launch action with the MPC controller: (a) engine and clutch speeds; (b) drive shaft torque; (c) clutch and engine torque; (d) active controller regions.

Rantzer and Johansson prove that a lower bound on the optimal cost can be estimated by solving a set of linear matrix inequalities (LMIs). Subsequently, an approximation for an optimal control law can be found. This control law is of the form

$$u(t) = \bar{L}_i \begin{bmatrix} x \\ 1 \end{bmatrix}, \quad x \in X_i, \quad i \in I \tag{26}$$

For more details, we refer to Rantzer and Johansson (2000) and Johansson (1999).

In the literature several extensions to this theory exist. In Solyom and Ranter (2002) the trajectory convergence of piecewise linear systems in presence of constant and time varying exogenous inputs is discussed. In Feng *et al.* (2002) H_∞ controller synthesis of piecewise linear systems is discussed. To our best knowledge, no examples of practical applications of the piecewise linear quadratic optimal control strategy are available in literature.

3.4.1 Design approach. The design of this controller is again based on the model discussed in § 3.2. However, in this case information on the engine speed ω_e is redundant. Also the dynamic behaviour of the combustion engine is taken into account, since it is relatively slow. The engine torque frequency response is modelled by a first order system

$$\dot{T}_e = \frac{1}{\tau}\hat{T}_e - \frac{1}{\tau}T_e \tag{27}$$

with τ the time constant of the dynamic system and $\hat{T}_e$ the new input. The new state and input vectors are then given by

$$x = \begin{pmatrix} (\omega_e - \omega_c) \\ \left(\dfrac{\omega_c}{i_{\text{tot}}} - \omega_v\right) \\ T_s \\ T_e \end{pmatrix}, \quad u = \begin{pmatrix} T_c \\ \hat{T}_e \end{pmatrix}. \tag{28}$$

The new system matrices are then given by equations (29) and (30).

Slip:

$$A_1 = \begin{pmatrix} 0 & \frac{b_s i_{\text{tot}}}{J_d} & \frac{i_{\text{tot}}}{J_d} & \frac{1}{J_e} \\ 0 & -\frac{b_s}{J_d} - \frac{b_s}{J_v} & -\frac{1}{J_d} - \frac{1}{J_v} & 0 \\ 0 & k_s & 0 & 0 \\ 0 & 0 & 0 & -\frac{1}{\tau} \end{pmatrix},$$

$$B_1 = \begin{pmatrix} -\frac{1}{J_e} - \frac{i_{\text{tot}}^2}{J_d} & 0 \\ \frac{i_{\text{tot}}}{J_d} & 0 \\ 0 & 0 \\ 0 & \frac{1}{\tau} \end{pmatrix} \tag{29}$$

Stick:

$$A_2 = \begin{pmatrix} 0 & 0 & 0 & 0 \\ 0 & -\frac{b_s}{J_{\text{tot}}} - \frac{b_s}{J_v} & -\frac{1}{J_{\text{tot}}} - \frac{1}{J_v} & \frac{i_{\text{tot}}}{J_{\text{tot}}} \\ 0 & k_s & 0 & 0 \\ 0 & 0 & 0 & -\frac{1}{\tau} \end{pmatrix},$$

$$B_2 = \begin{pmatrix} 0 & 0 \\ 0 & 0 \\ 0 & 0 \\ 0 & \frac{1}{\tau} \end{pmatrix}. \tag{30}$$

3.4.2 Reference trajectory generation. The approach discussed thus far is essentially a regulator design and does not consider a reference input or provide for command following. In order to do so, a new set of state variables and inputs is defined by

$$\left.\begin{aligned} \tilde{x}(t) &= x(t) - x_{\text{ref}}(t) \\ \tilde{u}(t) &= u(t) - u_{\text{ref}}(t) \end{aligned}\right\}, \tag{31}$$

where subscript "ref" denotes the reference value for the respective state/input.

We are only interested in prescribing a reference trajectory for drive shaft torque x_3, denoted by $r(t)$. By taking time derivatives of $r(t)$ and using the equations of motion of the reduced powertrain model, trajectories for the remaining state and input variables can be derived.

For the stick phase

$$\begin{aligned} r &= x_3 \\ \dot{r} &= \dot{x}_3 \\ &= k_s x_2 \\ \ddot{r} &= k_s \dot{x}_2 \\ &= k_s \left[-\left(\frac{b_s}{J_{\text{tot}}} + \frac{b_s}{J_v} \right) x_2 - \left(\frac{1}{J_{\text{tot}}} + \frac{1}{J_v} \right) x_3 + \frac{i_{\text{tot}}}{J_{\text{tot}}} x_4 \right] \\ &= k_s \left[-\frac{1}{k_s} \left(\frac{b_s}{J_{\text{tot}}} + \frac{b_s}{J_v} \right) \dot{r} - \left(\frac{1}{J_{\text{tot}}} + \frac{1}{J_v} \right) r + \frac{i_{\text{tot}}}{J_{\text{tot}}} x_4 \right] \\ x_{4,\text{ref}} &= \frac{J_{\text{tot}}}{k_s i_{\text{tot}}} \left[\ddot{r} + \left(\frac{b_s}{J_{\text{tot}}} + \frac{b_s}{J_v} \right) \dot{r} + \left(\frac{k_s}{J_{\text{tot}}} + \frac{k_s}{J_v} \right) r \right] \\ \dddot{r} &= k_s \left[-\frac{1}{k_s} \left(\frac{b_s}{J_{\text{tot}}} + \frac{b_s}{J_v} \right) \ddot{r} - \left(\frac{1}{J_{\text{tot}}} + \frac{1}{J_v} \right) \dot{r} + \frac{i_{\text{tot}}}{J_{\text{tot}}} \dot{x}_4 \right] \\ &= k_s \left[-\frac{1}{k_s} \left(\frac{b_s}{J_{\text{tot}}} + \frac{b_s}{J_v} \right) \ddot{r} - \left(\frac{1}{J_{\text{tot}}} + \frac{1}{J_v} \right) \dot{r} \right. \\ &\quad \left. + \frac{i_{\text{tot}}}{J_{\text{tot}}} \frac{1}{\tau} (-x_4 + u_2) \right] \\ u_{2,\text{ref}} &= \frac{J_{\text{tot}} \tau}{k_s i_{\text{tot}}} \left[\dddot{r} + \left(\frac{b_s}{J_{\text{tot}}} + \frac{b_s}{J_v} \right) \ddot{r} + \left(\frac{k_s}{J_{\text{tot}}} + \frac{k_s}{J_v} \right) \dot{r} \right] + x_{4,\text{ref}}. \end{aligned} \tag{32}$$

Similarly for the slip phase

$$\begin{aligned} r &= x_3 \\ \dot{r} &= \dot{x}_3 \\ &= k_s x_2 \\ \ddot{r} &= k_s \dot{x}_2 \\ &= k_s \left[-\left(\frac{b_s}{J_d} + \frac{b_s}{J_v} \right) x_2 - \left(\frac{1}{J_d} + \frac{1}{J_v} \right) x_3 + \frac{i_{\text{tot}}}{J_d} u_1 \right] \\ u_{1,\text{ref}} &= \frac{J_d}{k_s i_{\text{tot}}} \left[\ddot{r} + \left(\frac{b_s}{J_d} + \frac{b_s}{J_v} \right) \dot{r} + \left(\frac{k_s}{J_d} + \frac{k_s}{J_v} \right) r \right]. \end{aligned} \tag{33}$$

Note that by using this approach, reference trajectories for $x_{4,\text{ref}}$, $x_{1,\text{ref}}$ and $u_{2,\text{ref}}$ are not yet defined. Moreover, care should be taken to make sure that $x_{4,\text{ref}}$ (and hence $u_{2,\text{ref}}$ as well) is continuous when switching from slip to stick, in order to prevent oscillations in the driveline.

One possible approach would be to prescribe a reference trajectory for the engine rotational speed ω_e. A corresponding trajectory for $x_{4,\text{ref}}$ then follows from (11). Subsequently, values for $x_{1,\text{ref}}$ and $u_{2,\text{ref}}$ follow from the respective system equations. However, it is more convenient to choose $x_{1,\text{ref}} = 0$, since it can be freely chosen. Furthermore, the mode-switching should be dependent on x_1, rather than on $x_1 - x_{1,\text{ref}}$. This results in $u_{2,\text{ref,slip}} = u_{2,\text{ref,stick}}$.

3.4.3 Simulation results. The weight matrices Q_i and R_i are tuned in simulation. The objective here was to obtain a good transient behaviour for the nominal model, as well as a good robustness against variations in the clutch friction coefficient μ. A satisfactory performance was achieved with

$$Q_1 = \begin{bmatrix} 2 \cdot 10^{-3} & 0 & 0 & 0 \\ 0 & 1 \cdot 10^{3} & 0 & 0 \\ 0 & 0 & 2.5 \cdot 10^{3} & 0 \\ 0 & 0 & 0 & 1 \cdot 10^{-4} \end{bmatrix},$$

$$Q_2 = \begin{bmatrix} 1 \cdot 10^{-4} & 0 & 0 & 0 \\ 0 & 1 \cdot 10^{4} & 0 & 0 \\ 0 & 0 & 2.5 \cdot 10^{4} & 0 \\ 0 & 0 & 0 & 1 \cdot 10^{-2} \end{bmatrix},$$

$$R_1 = \begin{bmatrix} 2.5 \cdot 10^{-3} & 0 \\ 0 & 5 \cdot 10^{-2} \end{bmatrix},$$

$$R_2 = \begin{bmatrix} 2.5 \cdot 10^{-3} & 0 \\ 0 & 2.5 \cdot 10^{-3} \end{bmatrix}.$$

Resulting in

$$\bar{L}_1 = \begin{bmatrix} -0.0010 & -0.1701 & -17.7256 & -0.0064 & 1.07 \cdot 10^{-8} \\ -0.1999 & -5.1784 & -0.0179 & -0.1036 & 2.00 \cdot 10^{-6} \end{bmatrix},$$

$$\bar{L}_2 = \begin{bmatrix} 0 & 0 & 0 & 0 & 0 \\ 0.0052 & -103.5683 & -0.3581 & -2.0728 & 0 \end{bmatrix}.$$

Simulation results obtained with the PWLQ controller are depicted in figure 5. From these figures one can observe that the clutch closes very smoothly. All state variables follow their respective references very well and the resulting control action is relatively small. To demonstrate the robustness against variations in the clutch friction coefficient μ, the same simulations are done on a model with a friction coefficient of 0.4, instead of the nominal value of 0.2. The results are depicted in figure 6. From these figures, it can be seen that the controller reacts very well in this situation. Due to the higher friction coefficient, the clutch locks up somewhat earlier and more abrupt. However, oscillations in the drive shaft torque are well attenuated and overall the performance is still pretty good. It should be noted that a lower friction coefficient than the nominal one will always lead to a steady state offset in the slip speed of the clutch, which means that lock-up of the clutch will never be achieved. Instead, the clutch keeps slipping, causing unnecessary wear. It will therefore be necessary to add an integrator to the controller when this is to be implemented in a test vehicle.

4. Comparison with current control strategy

Now the PWLQ controller can be compared with a controller currently used by DTI. The latter is based on a PI controller and is depicted schematically in figure 7. It can be seen that the clutch torque T_c is used for closed-loop control of the engine speed ω_e. Here, C_2 denotes the PI controller. The reference engine speed is the maximum of (1) the desired engine launch speed $\omega_{e,\text{launch}}$, (2) the estimated engine idle speed $\omega_{e,\text{idle}}$ and (3) the clutch speed ω_c. The engine torque T_e is used for open-loop control of the drive shaft torque, denoted by C_1. The desired engine launch speed $\omega_{e,\text{launch}}$ and the reference drive shaft torque $T_{s,\text{ref}}$ are generated on the basis of the accelerator position. Hence, the drive shaft torque is not included in the control loop.

Simulation results obtained with this controller (used on the same powertrain model) are depicted in figure 8. From these results it can be seen that the clutch engages faster than with the PWLQ controller, yet still very smoothly. Unlike the PWLQ controller, this controller does not initially slow the engine down and hence the risk of stalling the engine is smaller. Regarding the drive shaft torque, it can be noticed that the high initial torque drops off to a lower value after some time (when ω_c surpasses $\omega_{e,\text{launch}}$). This is generally not appreciable in terms of "launch feel" (Serrarens *et al.* 2004). Also, a small delay in the response can be distinguished. The PWLQ controller does not exhibit this behaviour.

While the PI-based controller performs really well, it asks for a lot of ad-hoc tuning, both for the controller itself and for the generation of reference signals. Even more so when it is to be implemented in a test vehicle. The PWLQ controller, on the other hand, requires less tuning, albeit less intuitive.

Note that a more thorough comparison cannot be made at this point. This would require optimal tuning of the PI-based controller as well, according to a certain performance criterion. Therefore, it is not really possible to say if the PWLQ controller is better than the existing one.

5. Discussion

Now, the two design approaches presented in this paper can be compared. The behaviour of the MPC controller is largely determined by (physical) constraints. The behaviour of the PWLQ controller, on the other hand, is largely determined by the prescribed reference trajectories. Moreover, constraints on state and input variables are not taken into account with this method.

A consequence of the use of reference trajectories is that the generation of these trajectories becomes equally

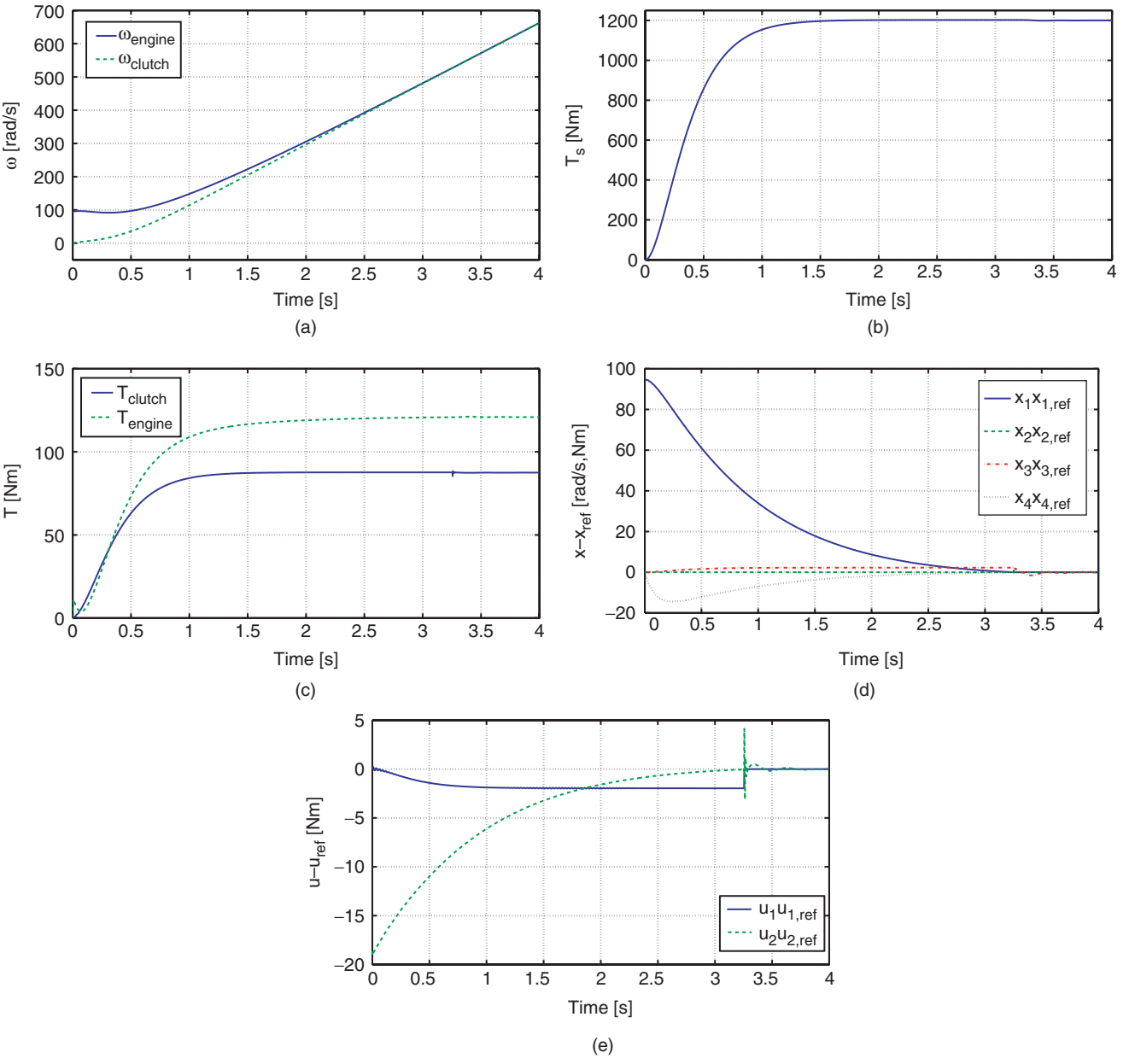

Figure 5. Launch action with the PWLQ controller (nominal μ of 0.2): (a) engine and clutch speeds; (b) drive shaft torque; (c) clutch and engine torque; (d) state variables; (e) control inputs.

important to the controller design. A whole new research can be devoted to this subject, but this is beyond the scope of this paper. It is possible to use tracking in combination with explicit MPC as well, but this yields a problem that is even harder to solve.

Regarding the computational costs, PWLQ is much faster and requires much less computing power than the explicit MPC method.

One could question the usefulness of the "hybrid" approach for this control problem. However, it is assumed that the added value of the piecewise linear approach over a standard linear LQR technique lies in the fact that the PWLQ controller automatically accounts for the switching from slip to stick, thereby preventing transitions that are too abrupt. Consequently, unwanted oscillations are prevented as well.

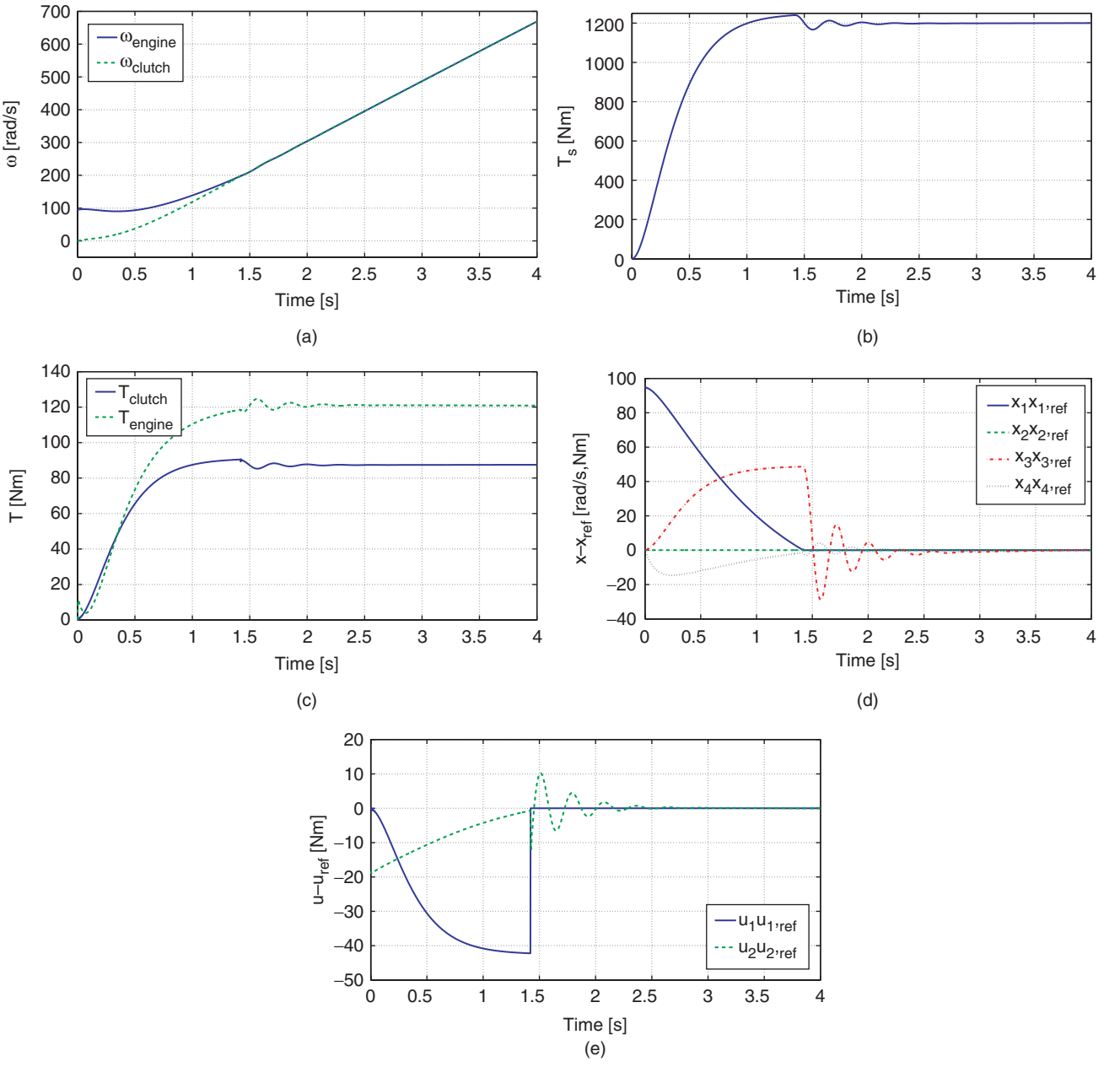

Figure 6. Launch action with the PWLQ controller ($\mu = 0.4$): (a) engine and clutch speeds; (b) drive shaft torque; (c) clutch and engine torque; (d) state variables; (e) control inputs.

Last but not least, it is recognized that by looking at the switching behaviour of the MPC controller, ideas for the design of switching or piecewise linear controllers can be gained.

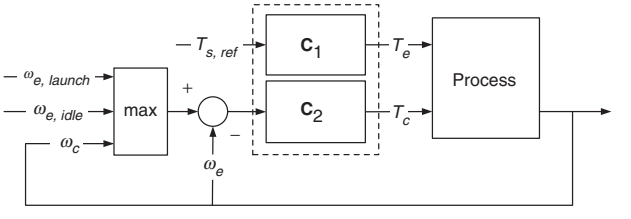

Figure 7. Control scheme of the PI-based controller.

6. Conclusions

Two optimal control strategies for the clutch engagement problem are presented. It can be concluded that

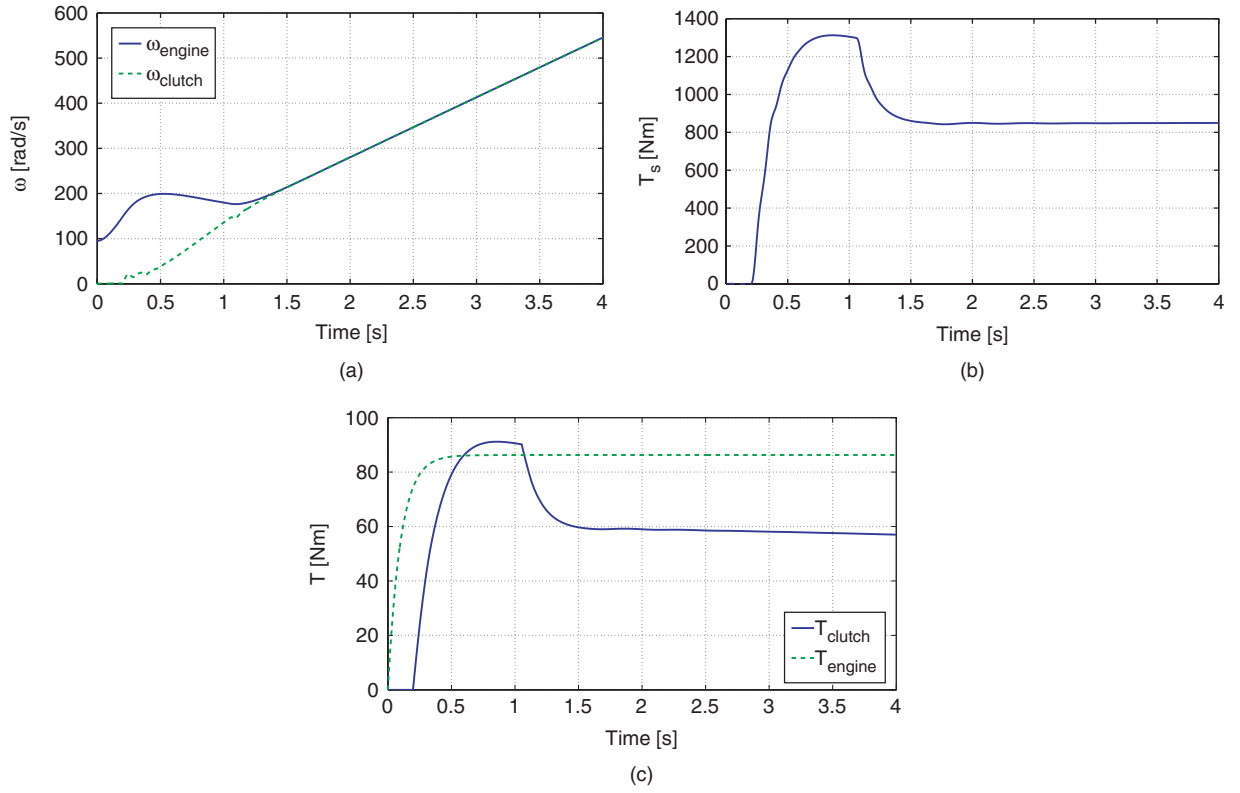

Figure 8. Launch action with PI-based controller: (a) engine and clutch speeds; (b) drive shaft torque; (c) clutch and engine torque.

explicit MPC is not suitable yet for these type of problems, mainly because of the large computational cost associated with it. However, it is a very promising technique and it may be of value in the future. PWLQ control, on the other hand, gives good results and is relatively easy and flexible in its use. In simulations it performs comparable to the PI-based controller, but requires less tuning.

So far the piecewise linear quadratic controller is only tested in simulation. It is planned to do experiments with this controller in a test vehicle. In the test vehicle all signals necessary for state feedback are directly available. However, in a production vehicle this is not the case and it is therefore suggested to investigate the possibilities of state estimation in further research.

Acknowledgement

This work was partially done in the framework of the HYCON Network of Excellence.

References

A. Bemporad, F. Borrelli and M. Morari, "Piecewise linear optimal controllers for hybrid systems", in *Proceedings of the American Control Conference*, Chicago, USA, 2000, pp. 1190–1194.

A. Bemporad, F. Borrelli, L. Glielmo and F. Vasca, "Hybrid control of dry clutch engagement", in *Proceedings of the European Control Conference*, Porto, Portugal, 2001a, pp. 635–639.

A. Bemporad, F. Borrelli, L. Glielmo and F. Vasca, "Optimal piecewise-linear control of dry clutch engagement", In *Proceedings of the IFAC Workshop: Advances in Automotive Control*, Karlsruhe, Germany, 2001b, pp. 33–38.

P. Dolcini, H. Béchart and C. Canudas de Wit, "Observer-based optimal control of dry clutch engagement", in *Proceedings of the 44th IEEE Conference on Decision and Control and the European Control Conference*, Seville, Spain, 2005, pp. 440–445.

G. Feng, G.P. Lu and S.S. Zhou, "An approach to H_∞ controller synthesis of piecewise linear systems", *Commun. Inform. Syst.*, 2, pp. 245–254, 2002.

L. Glielmo and F. Vasca, "Optimal control of dry clutch engagement", *SAE Technical Paper* 2000-01-0837, 2000.

M. Johansson, "Piecewise linear control systems", PhD thesis, Department of Automatic Control, Lund Institute of Technology, Sweden (1999).

M. Kvasnica, P. Grieder and M. Baotić, Multi-Parametric Toolbox (MPT), 2004. Available at http://control.ee.ethz.ch/~mpt/

H.B. Pacejka. *Tyre and Vehicle Dynamics*, Oxford: Butterworth-Heinemann Ltd, 2002.

A. Rantzer and M. Johansson, "Piecewise linear quadratic optimal control", *IEEE Trans. Automat. Contr.*, 45, pp. 629–637, 2000.

A.F.A. Serrarens, M. Dassen and M. Steinbuch, "Simulation and control of an automotive dry clutch", in *Proceedings of the American Control Conference*, Boston, USA, 2004, pp. 4078–4083.

S. Solyom and A. Rantzer, "The servo problem for piecewise linear systems", in *Proceedings of the Fifteenth International Symposium on Mathematical Theory of Networks and Systems*, Notre Dame, IN, August 2002.

The MathWorks, Inc. SimDriveline version 1.0.2, 2005.